

The fingerprint of binary intermediate mass black holes in globular clusters: supra-thermal stars and angular momentum alignment

M. Mapelli¹, M. Colpi², A. Possenti³ & S. Sigurdsson⁴

¹*S.I.S.S.A., Via Beirut 2 - 4, I-34014 Trieste, Italy; mapelli@sissa.it*

²*Dipartimento di Fisica G. Occhialini, Università di Milano Bicocca, Piazza della Scienza 3. I-20126 Milano, Italy;*

monica.colpi@mib.infn.it

³*INAF, Osservatorio Astronomico di Cagliari, Poggio dei Pini, Strada 54, 09012 Capoterra, Italy; possenti@ca.astro.it*

⁴*Department of Astronomy and Astrophysics, The Pennsylvania State University, 525 Davey Lab, University Park, PA 16802; steinn@astro.psu.edu*

24 December 2018

ABSTRACT

We propose a new approach to unveil the presence of binary intermediate mass black holes (IMBHs) in the core of globular clusters (GCs). We study the signature that a binary IMBH imprints on the velocity and on the angular momentum of cluster stars, simulating 3-body encounters between a star and a binary IMBH. We find that the binary IMBH generates a family of few hundreds of stars (~ 100 -300) which remain bound to the cluster and have velocity significantly higher than the dispersion velocity. For this reason we term them "supra-thermal" stars. We also notice that, after the interaction, a considerable fraction (55-70%) of stars tend to align their orbital angular momentum with the angular momentum of the binary IMBH, introducing an anisotropy in the angular momentum distribution of cluster stars. This phenomenon strongly depends on the reduced mass and on the orbital separation of the binary IMBH. We simulate the dynamical evolution of these supra-thermal stars before thermalization, and find that these stars tend to cluster at a distance of few core radii from the GC center. We, further, provide an estimate of the number of supra-thermal stars which can be detected through spectroscopic or photometric measurements. We conclude that the detection of these supra-thermal stars, even if quite difficult with present instrumentation, can provide an indication of the existence of a binary IMBH in the GC core. We shortly discuss angular momentum alignment and dynamical heating by a supermassive black hole binary on stars in a galactic nucleus.

Key words: black hole physics-globular clusters: general-stellar dynamics

1 INTRODUCTION

A number of different observations suggest that large black holes (BHs) may exist in nature, with masses between $20M_{\odot} - 10^4M_{\odot}$. Heavier than the stellar-mass BHs born in core-collapse supernovae ($3M_{\odot} - 20M_{\odot}$; Orosz 2002), these intermediate mass black holes (IMBHs) are expected to form from the direct collapse of very massive stars, or in dense stellar systems through complex dynamical processes. Filling the gap between stellar-mass black holes (BHs) and super-massive black holes (SMBHs), they are of crucial importance in establishing the potential physical link between these two classes.

IMBHs may plausibly have formed in the early universe as remnants of the first generation of metal free stars (Abel, Bryan & Norman 2002; Heger et al. 2003; Schneider et al.

2002). If this is true, IMBHs can participate the cosmic assembly of galaxies and be incorporated in larger and larger units, becoming seeds for the formation of SMBHs (Madau & Rees 2001; Volonteri, Haardt & Madau 2003). IMBH may still be forming in young dense star clusters vulnerable to unstable mass segregation, via collisions of massive stars (Portegies Zwart 2004; Portegies Zwart et al. 2004; Portegies Zwart & McMillan 2002; Gürkan et al. 2004; Freitag et al. 2005a, 2005b; see van der Marel 2004 for a review). Unambiguous detections of individual IMBHs do not exist yet, but there are observational hints in favor of their existence, from studies of ultra-luminous X-ray sources in nearby star-forming galaxies (Fabbiano 2004; Mushotzky 2004; Miller & Hamilton 2002).

It has also been long suspected that globular clusters (GCs) may hide IMBHs in their cores despite the fact

that their formation root is poorly known: runaway mergers among the most massive stars, at the time of cluster formation, can lead to an IMBH, similarly to what has been conjectured to occur in young dense star clusters (Portegies Zwart et al. 2004; Fregeau et al. 2004). An alternative pathway is based on the idea that IMBHs form later in the evolution of GCs through mergers of stellar-mass BHs. Segregating by dynamical friction in the core, these BHs are captured in binaries that form through dynamical encounters with stars and BHs. The picture is that hardening by subsequent interactions with BHs lead them to merge, emitting gravitational waves (Miller & Hamilton 2002). BHs more massive than stellar-mass BHs are thus created. However, the interactions that produce hardening also provide recoil, causing the ejection of BHs (Kulkarni, Hut & McMillan 1993; Sigurdsson & Hernquist 1993; Portegies Zwart & McMillan 2000), but the heaviest black holes may remain, if their mass exceeds a still uncertain value between $\sim 50M_{\odot}$ and $\sim 300M_{\odot}$ (Miller & Hamilton 2002; Colpi, Mapelli & Possenti 2003; Gultekin, Miller & Hamilton 2004).

At present, optical observations of GCs hint in favor of the existence of IMBHs. In particular Gebhardt, Rich & Ho (2002) suggest the presence of a $2_{-0.8}^{+1.4} \times 10^4 M_{\odot}$ IMBH, to explain the kinematics and the surface brightness profile of the globular cluster G1 in M31. Gerssen et al. follow the same method to indicate the possible presence of a $1.7_{-1.7}^{+2.7} \times 10^3 M_{\odot}$ IMBH in the galactic globular cluster M15 (Gerssen et al. 2002, 2003). In addition, there has been some claim of the existence of rotation in the core of a few GCs (Gebhardt et al. 1995; Gebhardt et al. 1997; Gebhardt et al. 2000) suggesting the presence of a steady source of angular momentum in their cores.

Radio observations can also help in discovering concentrations of under-luminous matter in the core of GCs, thanks to the presence of millisecond pulsars that can probe the underlying gravitational field of the cluster. Currently, there are more than 100 known millisecond pulsars in GCs (Possenti 2003; Ransom et al. 2005; Camilo & Rasio 2005) and some show large and negative period derivatives. This is an important peculiarity, because millisecond pulsars spin down intrinsically due to magnetic braking. Negative period derivatives come from the variable Doppler shift caused by the acceleration of the pulsar in the gravitational field of the cluster itself (Phinney 1993). When these negative period derivatives can be ascribed solely to the gravitational field of the cluster, these pulsars place a lower limit on the mass enclosed inside their projected distance from the globular cluster center.

Two pulsars in M 15, at 1" from the core were found (Phinney 1993) with negative values of their period derivatives, consistent with the mass distribution implied by the stellar kinematics. The recent discovery by D'Amico et al. (2002) of two accelerated pulsars in NGC 6752 at 6" and 7" from the center has highlighted the presence of about $2 \times 10^3 M_{\odot}$ of under-luminous matter in the core of the cluster (Ferraro et al. 2003), making NGC 6752 a special target for the search of an IMBH. NGC 6752 is interesting also because it hosts two pulsars in its halo. PSR-A is a millisecond pulsar in a binary system with a white dwarf (Ferraro et al. 2003), located at 3.3 half mass radii away: it is the farthest pulsar ever observed in a cluster. Colpi, Possenti & Guadrandis (2002), and Colpi, Mapelli & Possenti (2003, 2004)

have suggested that this pulsar has been propelled in the halo due to a dynamical interaction with a binary IMBH. In modeling the gravitational encounter, Colpi, Mapelli & Possenti (2003) found that a (50–200, 10) M_{\odot} binary IMBH is the preferred target for imprinting the large kick to the pulsar. Colpi et al. (2005) shortly reviewed the dynamical effects that a binary IMBH would imprint on cluster stars.

Considering all the recent hints provided by optical and radio observations, we propose, in this paper, a new way to unveil a binary IMBH in a GC, previously overlooked, that exploits the dynamical fingerprint left by a binary IMBH on cluster stars. In particular we like to address a number of questions: (i) What signature does a binary IMBH imprint on cluster stars? Are the stars heated during the scattering process still remaining bound to the cluster? (ii) Is there direct transfer of angular momentum from the binary IMBH to the stars to produce some degree of alignment, given the large inertia of the BHs? (iii) Are prograde or retrograde orbits equally scattered?

In this paper, we simulate 3-body encounters of cluster stars with a binary IMBH, studying the energy and angular momentum exchange, and, reconstructing the trajectories of those stars that are scattered away from equilibrium by the binary IMBH. In Section 2 we outline the method used to simulate 3-body encounters between a binary IMBH and the cluster stars. In Section 3, we present our main results: the formation, in a GC dynamically dominated by a binary IMBH, of a population of high velocity (bound) stars (that we call "supra-thermal stars"), which tend to align their orbital angular momentum with that of the binary IMBH. In Section 4, we investigate on the detection of these supra-thermal stars. In particular, we use an upgraded version of the code presented in Sigurdsson & Phinney (1995) to follow the dynamical evolution of these supra-thermal stars inside a GC model which reproduces the characteristics of NGC 6752. This study allows us to put some constraint on the detection of this family of high velocity stars. Section 5 contains our conclusions.

2 THE SIMULATIONS

We simulated 3-body encounters involving a binary IMBH (composed of two BHs of mass M_1 and M_2) and a cluster star of mass $m = 0.5M_{\odot}$. The dynamics of the encounter is followed solving the equations of motion with a numerical code based on a Runge-Kutta fourth order integration scheme with adaptive stepsize and quality control (explained in Colpi, Mapelli & Possenti 2003, hereafter CMP). For the target binary IMBH we considered an interval of masses between $60M_{\odot}$ up to $210M_{\odot}$. These are the favored masses of the hypothetical binary IMBH in NGC 6752. The binary has semi-major axis a of 1, 10, 100, and 1000 AU and eccentricity $e = 0.7$; the set of models is described in Table 1.

The initial conditions, that are Monte Carlo generated as in CMP, are sampled using the prescriptions indicated in Hut & Bahcall (1983). In particular, the impact parameter b is drawn at random from a probability distribution uniform in b^2 and the relative velocity u^{in} is distributed homogeneously between $8.5 - 11 \text{ km s}^{-1}$ (according to the value of stellar velocity dispersion measured in NGC 6752 which is

our reference cluster; Dubath, Meylan & Mayor 1997). We terminate (initiate) integration when the distance between the outgoing (incoming) star and the center of mass of the binary is comparable to the radius of gravitational influence of the IMBHs ($r_a \sim 2G(M_1 + M_2)/\sigma^2$, where σ is the 1-D stellar dispersion velocity). To classify the binary, we define the hardness parameter $h = E_{\text{BH}}/k_B T$ (given in Table 2), where $E_{\text{BH}} = GM_1 M_2/(2a)$ is the binding energy of the binary and $T \sim (3/2)m\sigma^2/k_B$.

At the end of every scattering experiment we store the final binding energy $E_{\text{BH}}^{\text{fin}}$ and angular momentum $\mathbf{J}_{\text{BH}}^{\text{fin}}$ of the binary IMBH, together with the post-encounter velocity u^{fin} and angular momentum $\mathbf{J}_*^{\text{fin}}$ of the interacting star. In this paper we want, in particular, to quantify the mean change in the absolute value J_* of the vector \mathbf{J}_* and the extent of alignment of \mathbf{J}_* in the direction of \mathbf{J}_{BH} .

3 RESULTS

3.1 Supra-thermal stars

We find that a sizable number of high velocity stars is created, under certain conditions, that may highlight the presence of an IMBH in the cluster. These stars gain kinetic energy and an excess velocity relative to the mean, remaining bound to the cluster. In Table 3 we give the fraction of bound stars, defined as those having a final velocity lower than the escape velocity from the core $\sim 35\text{-}40 \text{ km s}^{-1}$, and the fraction of high velocity or *supra-thermal* stars, defined as having a post-encounter speed between 20 and 40 km s^{-1} . Depending on the hardness of the binary IMBH, these stars can account for $\lesssim 50\%$ of all stars that have experienced an encounter.

Figure 1 shows the post-encounter velocity distribution of stars scattering off a binary IMBH, for cases D1, D2, D3 and D4 (in Table 1). The shaded area indicates the strip of supra-thermal stars. The mean values of the post-encounter velocity u^{fin} and of the fractional binding energy exchange $\Delta E_{\text{BH}}/E_{\text{BH}}^{\text{in}} = (E_{\text{BH}}^{\text{fin}} - E_{\text{BH}}^{\text{in}})/E_{\text{BH}}^{\text{in}}$ are given in Table 2 together with the dimensionless factor ξ_E , defined by:

$$\Delta E_{\text{BH}}/E_{\text{BH}}^{\text{in}} = \xi_E [m/(M_1 + M_2)]. \quad (1)$$

As illustrated in Figure 1, dynamical encounters widen the velocity distribution of the stars. This effect is particularly severe when the binary is hard, having a higher binding energy which becomes available in the interaction. ξ_E clusters around values between 0.6 and 4, and shows a maximum declining as the binary becomes extremely hard. This explains why case D1 has a peak post-encounter velocity smaller than case D2 corresponding to a less hard binary (see Table 2). We tried to fit the behavior of ξ_E , as a function of the orbital separation a , with a parabola. We obtained $\xi_E = b \text{Log}^2(a) + c \text{Log}(a) + d$ for $b = -1.2495$, $c = 3.8615$, $d = 0.958$; this fit is only an approximation, since we have few numerical points (Fig. 2).

In Figure 1, case D1 and D3 give the highest number of supra-thermal stars among the different runs. These supra-thermal stars are the ones that have also acquired a sizable fraction of the orbital angular momentum of the binary IMBH. Thus in scattering off the binary IMBH they are preferentially launched in a halo orbit, inside the cluster.

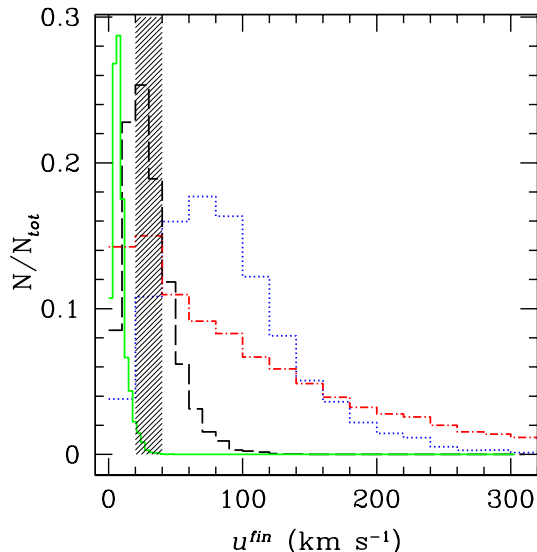


Figure 1. Post-encounter velocity distributions of the cluster star in the case D1 (dotted-dashed line), D2 (dotted line), D3 (dashed line), D4 (solid line). The shaded area refers to the supra-thermal stars. On the y-axis the number of cases for each bin is normalized to the total number of resolved runs (N_{tot}).

Their detection (discussed in § 4) would be the sign of an IMBH hidden in the cluster.

3.2 Angular Momentum Transfer and Alignment

An interesting question to address is whether and how the orbital angular momentum of the binary IMBH couples to the star after a close gravitational encounter. The BHs can be sufficiently massive and the orbit be sufficiently wide that the orbital angular momentum of the binary exceeds that of the incoming star. In this case a direct transfer of orbital angular momentum can occur. The star coming close to the binary IMBH can be dragged into corotation, i.e. the star can emerge after the encounter with an angular momentum nearly aligned with the binary IMBH.

If we denote with $\mu = M_1 M_2/(M_1 + M_2)$ the reduced mass of the binary hosting the two BHs, the total angular momentum of the system is

$$\mathbf{J} = \mathbf{J}_{\text{BH}}^{\text{in}} + \mathbf{J}_*^{\text{in}} = \mu \sqrt{a G (M_1 + M_2)} \mathbf{z} + b u^{\text{in}} \left[\frac{m(M_1 + M_2)}{M_1 + M_2 + m} \right] \mathbf{z}' \quad (2)$$

where \mathbf{z} and \mathbf{z}' are the unit vectors indicating respectively the directions of $\mathbf{J}_{\text{BH}}^{\text{in}}$ and \mathbf{J}_*^{in} . Angular momentum transfer from the binary to the interacting star and partial alignment become important when $J_{\text{BH}}^{\text{in}} > J_*^{\text{in}}$, i.e., when

$$\frac{\mu}{b u^{\text{in}} m} \sqrt{(M_1 + M_2) a G} \gg 1. \quad (3)$$

Our experiment confirms this fact. Figure 3 (solid lines) shows the post-encounter distribution of J_* for cases D2, D3 and D4. It is compared with the distribution of J_* of the incoming stars (dashed lines) to show that the binary IMBH transfers angular momentum to the stars widening the distribution of J_* . Table 2 contains the averaged value

Table 1. Initial Parameters.

	M_1^a	M_2^a	Semi-major axis (a) ^b	Range of impact parameters ^b	Number of simulations
CASE A1	50	10	1	0-60	5000
CASE A2	50	10	10	0-60	10000
CASE A3	50	10	100	0-100	10000
CASE A4	50	10	1235	0-1000	10000
CASE B1	50	50	1	0-100	5000
CASE B2	50	50	10	0-100	5000
CASE B3	50	50	100	0-100	5000
CASE B4	50	50	1000	0-1000	5000
CASE C1	100	10	1	0-100	5000
CASE C2	100	10	10	0-100	5000
CASE C3	100	10	100	0-100	5000
CASE C4	100	10	1000	0-1000	5000
CASE D1	100	50	1	0-100	5000
CASE D2	100	50	10	0-100	5000
CASE D3	100	50	100	0-100	5000
CASE D4	100	50	1000	0-1000	5000
CASE E1	200	10	1	0-100	5000
CASE E2	200	10	10	0-100	5000
CASE E3	200	10	100	0-100	5000
CASE E4	200	10	1000	0-1000	5000

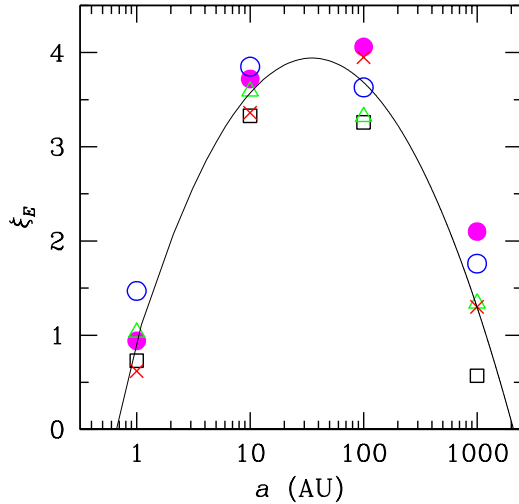
^a In units of the solar mass.^b In Astronomical Units.

Figure 2. $\xi_E \equiv [(M_1 + M_2)/m][\Delta E_{BH}/E_{BH}^{in}]$ as a function of the orbital separation a for all the considered cases. A1, A2, A3 and A4 are represented by *open triangles*; B1, B2, B3 and B4 by *crosses*; C1, C2, C3 and C4 by *open squares*; D1, D2, D3 and D4 by *filled circles*; E1, E2, E3 and E4 by *open circles*. The *solid line* indicates a parabolic fit $b \text{Log}^2(a) + c \text{Log}(a) + d = \xi_E(a)$, where $b=-1.2495$, $c=3.8615$, $d=0.958$.

of the fractional angular momentum increase (in modulus) $\Delta J_*/J_*^{in}$ for the complete series of runs. $\Delta J_*/J_*^{in}$ is large and exceeds unity in correspondence to the runs where the

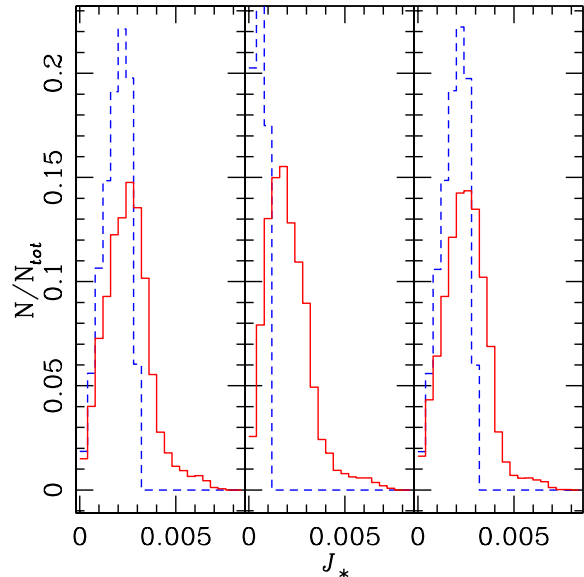


Figure 3. Angular momentum distribution of the cluster star in the case D2 (*left panel*), D3 (*central panel*), D4 (*right panel*). The angular momenta are in dimensionless units (i.e. normalized to the length, mass and time scales). *Dashed line* indicates the initial angular momentum distribution, *solid line* indicates the post-encounter angular momentum distribution. Evidence of angular momentum transfer from the binary to the cluster star occurs when the binary has a semi-major axis of 100 AU (case D3); while the softest binary (case D4, $a=1000$ AU) is the least efficient from this point of view. On the y-axis the number of cases for each bin is normalized to the total number of resolved runs (N_{tot}).

Table 2. Final velocities and angular momentum exchanges.^a

	h^b	$u^{fin}{}^c$	$\langle \frac{\Delta J}{J_*} \rangle^d$	$\frac{\Delta J}{J_*}^e$	ξ_J^f	$\langle \frac{\Delta E}{E_{BH}^{in}} \rangle^g$	ξ_E^h
CASE A1	12280	$12.5^{+95.0}_{-10.0}$	$0.056^{+14.40}_{-0.054}$	$0.025^{+0.100}_{-0.100}$	-0.066	$0.0086^{+0.4520}_{-0.0073}$	1.03
CASE A2	1228	$37.5^{+35.0}_{-30.0}$	$0.630^{+8.24}_{-0.592}$	$0.175^{+1.150}_{-0.850}$	-0.21	$0.0299^{+1.1032}_{-0.0186}$	3.59
CASE A3	123	$12.5^{+10.0}_{-10.0}$	$1.12^{+1.82}_{-1.13}$	$0.725^{+2.200}_{-1.400}$	-0.25	$0.0277^{+1.0363}_{-0.0191}$	3.32
CASE A4	10	$7.5^{+2.0}_{-3.0}$	$0.155^{+30.330}_{-0.228}$	$0.025^{+0.350}_{-0.500}$	-0.02	$0.0112^{+0.0309}_{-0.0199}$	1.34
CASE B1	61410	$12.5^{+75.0}_{-12.5}$	$0.037^{+7.980}_{-0.037}$	$0.005^{+0.020}_{-0.005}$	-0.01	$0.0031^{+0.1778}_{-0.0030}$	0.62
CASE B2	6141	$67.5^{+60.0}_{-55.0}$	$0.317^{+31.840}_{-0.346}$	$0.025^{+0.65}_{-0.55}$	-0.17	$0.0168^{+0.2621}_{-0.0109}$	3.36
CASE B3	614	$17.5^{+25.0}_{-15.0}$	$1.994^{+145.935}_{-1.456}$	$0.325^{+2.850}_{-1.100}$	-0.21	$0.0198^{+0.2255}_{-0.0134}$	3.95
CASE B4	61	$8.5^{+3.0}_{-6.0}$	$0.197^{+17.279}_{-0.259}$	$-0.0255^{+0.550}_{-0.400}$	-0.17	$0.0065^{+0.0150}_{-0.0073}$	1.30
CASE C1	24560	$12.5^{+60.0}_{-10.0}$	$0.020^{+5.726}_{-0.020}$	$0.005^{+0.010}_{-0.005}$	-0.02	$0.0033^{+0.7152}_{-0.0032}$	0.73
CASE C2	2456	$32.5^{+40.0}_{-25.0}$	$0.154^{+0.891}_{-0.284}$	$0.075^{+0.550}_{-0.550}$	-0.08	$0.0151^{+0.4422}_{-0.0095}$	3.33
CASE C3	246	$12.5^{+10.0}_{-10.0}$	$0.876^{+1.639}_{-1.135}$	$0.520^{+3.200}_{-1.040}$	-0.12	$0.0148^{+0.5524}_{-0.0098}$	3.26
CASE C4	25	$5.9^{+2.5}_{-3.1}$	$0.212^{+21.888}_{-0.255}$	$0.025^{+0.500}_{-0.500}$	-0.02	$0.00261^{+0.00911}_{-0.00773}$	0.57
CASE D1	122820	$30.0^{+160.0}_{-30.0}$	$0.062^{+12.175}_{-0.059}$	$0.005^{+0.090}_{-0.050}$	-0.02	$0.0031^{+0.1054}_{-0.0027}$	0.94
CASE D2	12282	$75.0^{+70.0}_{-60.0}$	$0.205^{+0.703}_{-0.623}$	$0.225^{+0.850}_{-1.000}$	-0.18	$0.0124^{+0.1679}_{-0.0078}$	3.72
CASE D3	1228	$22.5^{+30.0}_{-20.0}$	$2.911^{+7.894}_{-1.801}$	$1.235^{+3.780}_{-1.890}$	-0.28	$0.0135^{+0.0348}_{-0.0090}$	4.06
CASE D4	123	$7.0^{+6.0}_{-6.0}$	$0.384^{+1.243}_{-0.512}$	$0.185^{+1.050}_{-0.840}$	-0.18	$0.0070^{+0.7796}_{-0.0065}$	2.10
CASE E1	49130	$27.5^{+105.0}_{-25.0}$	$0.025^{+7.087}_{-0.024}$	$0.005^{+0.050}_{-0.030}$	-0.01	$0.0035^{+0.7193}_{-0.0027}$	1.47
CASE E2	4913	$32.5^{+45.0}_{-25.0}$	$0.429^{+28.250}_{-0.381}$	$0.065^{+0.540}_{-0.420}$	-0.02	$0.0092^{+0.6392}_{-0.0058}$	3.85
CASE E3	491	$13.5^{+12.0}_{-12.0}$	$1.212^{+3.718}_{-0.881}$	$0.675^{+1.350}_{-1.700}$	-0.03	$0.0086^{+0.6697}_{-0.0060}$	3.63
CASE E4	49	$6.5^{+3.0}_{-5.0}$	$0.395^{+50.771}_{-0.347}$	$0.075^{+0.450}_{-0.400}$	-0.03	$0.0042^{+0.0191}_{-0.0067}$	1.76

^a We consider both bound and ejected stars. Only unresolved encounters are neglected in this Table.

^b hardness parameter $h \equiv E_{BH}/k_B T$.

^c In units of km s^{-1} . Peak value of the post-encounter velocity of the star cluster. The dispersion around the peak value is calculated considering those values which contain 50% of the total area descending from the peak.

^d $\Delta J \equiv (J_*^{fin} - J_*^{in})$, where J_*^{in} and J_*^{fin} represent respectively the modulus of the initial and the final angular momentum of the cluster star. $\langle \frac{\Delta J}{J_*} \rangle$ is the mean value of the variation of the absolute value of the angular momentum of the cluster star, normalized to its initial value J_*^{in} . The dispersion around the mean value is calculated considering those values which contain 34% of the total area in the left and right wings, respectively.

^e $\frac{\Delta J}{J_*}$ is the peak value of $\frac{\Delta J}{J_*}$. The dispersion around the peak value is calculated considering those values which contain 50% of the total area descending from the peak.

^f ξ_J is given by $\xi_J \equiv \frac{\mu}{m} \langle \frac{\Delta J_{BH}}{J_{BH}^{in}} \rangle$, considering only bound outcoming stars.

^g $\langle \frac{\Delta E}{E_{BH}^{in}} \rangle$ is the mean value of the variation of the binding energy of the binary IMBH, normalized to its initial binding energy E_{BH}^{in} .

The dispersion around the mean value is calculated considering those values which contain 34% of the total area in the left and right wings, respectively.

^h ξ_E represents the hardening factor and is given by $\xi_E \equiv \frac{M_1 + M_2}{m} \langle \frac{\Delta E}{E_{BH}^{in}} \rangle$ (CMP 2003).

bulk of the supra-thermal stars are produced. It has a non monotonic trend with the hardness parameter h : a harder binary has little excess of angular momentum in its initial state relative to that of the incoming star; so the efficiency of angular momentum transfer reduces. A less hard binary (having a larger J_{BH}^{in}) is also less efficient, since it does not alter much the post-encounter velocity. If we introduce the dimensionless factor ξ_J

$$\Delta J_{BH}/J_{BH}^{in} = \xi_J (m/\mu), \quad (4)$$

we can measure the extent of angular momentum transfer from the binary IMBH to the star. Table 2 collects the values of ξ_J averaged over all runs.

We can further quantify the importance of angular momentum transfer from the binary to the star, by computing

the fraction of stars which increase J_* after an interaction; this is given in the last column of Table 4. The fraction of stars that do so, over the total (in the sample of the bound stars), is significantly high: it is above 70% in many cases.

Is alignment induced in the scattering process? In Table 4 we compare the percentage of bound stars which were corotating (i.e. for which the scalar product between their angular momentum and the angular momentum of the binary is positive, that is $\mathbf{J}_* \cdot \mathbf{J}_{BH} > 0$) before the 3-body interaction with the percentage of those stars which are corotating after the 3-body interaction. Whereas the fraction of corotating stars before the interaction is $\sim 50\%$ (as one can expect given the initial sampling of the data), the fraction of corotating stars after the interaction is often over 60%, indicating a tendency of stars to align their angular

Table 3. Statistics of the Outgoing States.

	Bound stars (%)	Ejections (%)	Unresolved Encounters (%)	Supra-thermal stars (%) ^a
CASE A1	45.02	53.12	1.86	21.46
CASE A2	51.32	47.10	1.58	35.56
CASE A3	97.60	1.65	0.75	17.23
CASE A4	99.98	0.00	0.02	0.06
CASE B1	53.78	43.44	2.78	13.12
CASE B2	21.12	77.90	0.98	15.58
CASE B3	83.36	16.30	0.34	43.36
CASE B4	99.96	0.00	0.04	0.36
CASE C1	60.46	34.82	4.72	15.10
CASE C2	51.30	45.58	3.12	35.24
CASE C3	95.56	1.80	2.64	17.22
CASE C4	99.86	0.00	0.14	0.01
CASE D1	28.04	67.84	4.12	14.38
CASE D2	14.44	84.18	1.38	10.68
CASE D3	75.20	24.32	0.48	44.04
CASE D4	99.84	0.04	0.12	3.46
CASE E1	27.60	62.54	9.86	17.86
CASE E2	45.84	47.42	6.74	31.54
CASE E3	88.68	2.36	8.96	18.42
CASE E4	98.48	0.02	1.50	0.38

^a We define supra-thermal stars those with post-encounter velocities comprised between 20 and 40 km s⁻¹.

Table 4. Statistics for bound stars^a.

	Corot _{in} (%) ^b	Corot _{fin} (%) ^c	More aligned stars (%) ^d	$J_*^{fin} > J_*^{in}$ (%) ^e
CASE A1	40	42	52	64
CASE A2	47	59	61	72
CASE A3	49	68	65	87
CASE A4	50	51	50	55
CASE B1	46	46	50	59
CASE B2	57	63	53	64
CASE B3	50	58	56	83
CASE B4	50	58	55	58
CASE C1	46	46	51	59
CASE C2	45	49	58	64
CASE C3	49	62	64	88
CASE C4	50	52	51	59
CASE D1	40	40	51	64
CASE D2	55	60	52	71
CASE D3	51	70	62	95
CASE D4	50	69	63	71
CASE E1	40	40	50	61
CASE E2	42	45	60	65
CASE E3	48	53	61	92
CASE E4	50	54	59	63

^a In this Table we consider only the stars which after the interaction with the binary remain bound to the cluster.

^b Corot_{in} ≡ corotating stars before the interaction. Percentage (respect to the total of bound stars) of stars which, before the interaction, are corotating with the binary (i.e. for which the scalar product between their angular momentum and the angular momentum of the binary is positive). As one must expect, they are near the 50% .

^c Corot_{fin} ≡ corotating stars after the interaction. Percentage (respect to the total of bound stars) of stars which, after the interaction, are corotating with the binary, independently from the initial orientation of their angular momentum.

^d Percentage of bound stars which, after the encounter, reduce the angle between their angular momentum and that of the binary.

^e Percentage of bound stars which, after the encounter, increase the absolute value of their angular momentum.

momentum with that of the binary IMBH. This tendency is greater if the binary has a big reduced mass (cases with $M_1 = 100, M_2 = 50 M_\odot$ and with $M_1 = 50, M_2 = 50 M_\odot$) and if the binary is moderately hard (i.e. its orbital separation is neither too small, because in this case $J_{\text{BH}}^{\text{in}}$ is comparable with J_*^{in} , nor too large, since in this case the binary would be too soft, and so the kinetic energy exchange would be negligible). In case D3 the bound stars which after the interaction are corotating with the binary are $\sim 70\%$. This means that we can observe a family of supra-thermal stars which have an anisotropy in their orbital angular momentum relative to the center of the cluster, 70% of them rotating in one direction and the remaining 30% rotating in the other. Obviously, we have to take into account that orbits initially are isotropically distributed and that we observe them in projection; then the detection of this phenomenon is not so immediate.

To better constrain orbit alignment in the direction of \mathbf{J}_{BH} , we considered separately orbits which before the encounter (as initial condition) were corotating (Table 5) and orbits which before the encounter were counterrotating (Table 6). For both we investigated the final distributions, and in particular we compared the fraction of stars initially corotating which after the interaction remain corotating (Table 5, 2nd column) with the fraction of stars initially counterrotating which after the interaction become corotating (Table 6, 2nd column). We found that most (at least 70%) of the initially corotating stars remains corotating, even if during very energetic interactions -with the hardest binaries- the star tends to forget its initial angular momentum orientation (case D2). In contrast, a high percentage of initially counterrotating stars becomes corotating, flipping their angular momentum. The combination of these two tendencies (i.e. the tendency to remain corotating for initially corotating stars and the tendency to become corotating for initially counterrotating stars) provides the strongest evidence of an alignment between $\mathbf{J}_{\text{BH}}^{\text{in}}$ and \mathbf{J}_*^{in} after the interaction (Fig. 4). In Fig. 5 we give a complete overview of the cases considered.

4 DETECTING SUPRA-THERMAL STARS

4.1 Estimating the number of supra-thermal stars

A measurable number of stars with anomalously high velocities would be one fingerprint left by a binary IMBH. A key question to address is whether this signature is observable. In particular, we would like to know if these stars are present in a sufficiently large number in a cluster not to be buried in the fluctuations of the velocity distribution of background stars. Since these supra-thermal stars have excess kinetic energy and angular momentum, they are not in dynamical equilibrium. Thus, two-body relaxation will try to obliterate such anisotropies. Friction will return them to the core where they become unrecognizable, unless some memory of the angular momentum alignment (e.g. Section 3.2) is retained during the relaxation process.

The first condition for detecting supra-thermal stars is constrained by:

- (i) the survival of the IMBH as a binary in the cluster core;

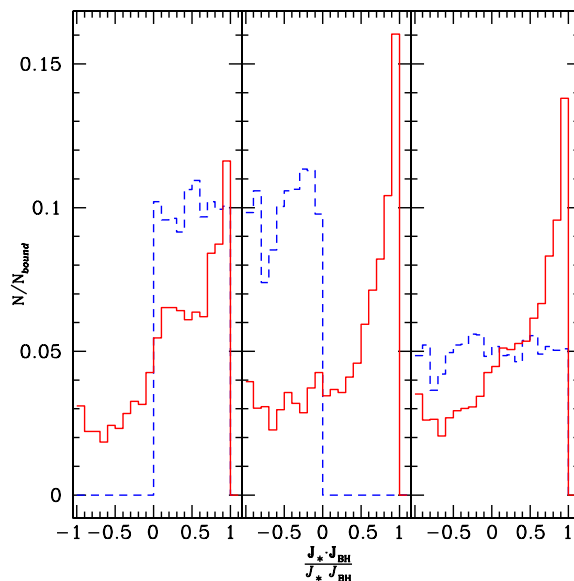


Figure 4. The histograms show the distribution of $\frac{\mathbf{J}_* \cdot \mathbf{J}_{\text{BH}}}{J_* J_{\text{BH}}}$ for the case D3 ($M_1 = 100 M_\odot, M_2 = 50 M_\odot, a = 100 \text{ AU}$). *Solid line* indicates the distribution after the encounter; *dashed line* indicates the distribution before the encounter. The left panel represents the distribution of $\frac{\mathbf{J}_* \cdot \mathbf{J}_{\text{BH}}}{J_* J_{\text{BH}}}$ for bound stars which before the encounter were corotating, the central panel the distribution for bound stars which before the encounter were counterrotating and the right panel the sum of the two distributions, i.e. the distribution for all the stars which after the encounter remain bound to the cluster. On the y-axis the number of cases for each bin is normalized to the total number of bound stars (N_{bound}).

- (ii) the persistence of the supra-thermal stars in the GC halo.

We can investigate these questions through a comparison between relevant timescales. The first timescale to consider is the hardening time of the binary IMBH, given the stellar number density in the core n and the binary separation a

$$t_{\text{hard}} = \frac{\sigma}{2\pi a \xi_E G m n} \quad (5)$$

The second relevant timescale is the relaxation time at the half mass radius

$$t_{rh} = \frac{0.14N}{\ln(0.4N)} \left(\frac{r_h^3}{GM} \right)^{1/2} \quad (6)$$

where N and M are respectively the number of stars and the total mass of the cluster. In Figure 6 we compare the two timescales for $\sigma = 8.5 \text{ km s}^{-1}$, $\xi_E \sim 1$ (see Table 2) and $n = 10^5 \text{ stars pc}^{-3}$. This plot shows that, when the binary is not very hard, i.e., when $a > 4 \text{ AU}$, the hardening time is shorter than the half-mass relaxation time. This implies that we can simultaneously observe all the supra-thermal stars in the halo for a time comparable to t_{rh} with no dilution. On the other hand, when the binary has orbital separation $a \leq 4 \text{ AU}$, t_{rh} is shorter than t_{hard} , and, then, we can not simultaneously observe all the produced supra-thermal stars in the halo, a part of them being already thermalized. However, this effect is balanced by the fact that the binary remains in this very hard configuration

Table 5. Statistics for initially corotating bound stars^a.

	Corot _{fin} (%) ^b	Counterrot _{fin} (%) ^c	More aligned stars (%) ^d	$J_*^{fin} > J_*^{in}$ (%) ^e
CASE A1	93	7	49	70
CASE A2	77	23	44	77
CASE A3	79	21	48	90
CASE A4	82	18	42	53
CASE B1	97	3	50	63
CASE B2	67	33	34	67
CASE B3	60	40	35	84
CASE B4	62	38	33	61
CASE C1	98	2	50	62
CASE C2	81	19	46	73
CASE C3	86	14	48	91
CASE C4	86	14	45	60
CASE D1	92	8	50	68
CASE D2	65	35	31	67
CASE D3	72	28	41	93
CASE D4	75	25	43	71
CASE E1	94	6	48	63
CASE E2	86	14	48	73
CASE E3	96	4	35	95
CASE E4	94	6	53	70

^a In this Table we consider only the stars which before the interaction were corotating.

^b Percentage (respect to the total of initially corotating bound stars) of stars which, after the interaction, remain corotating with the binary.

^c Percentage (respect to the total of initially corotating bound stars) of stars which, after the interaction, become counterrotating respect to the binary.

^d Percentage (respect to the total of initially corotating bound stars) of stars which, after the encounter, reduce the angle between their angular momentum and that of the binary.

^e Percentage of bound stars (respect to the total of initially corotating bound stars) which, after the encounter, increase the absolute value of their angular momentum.

for most of its life, and, therefore, we can observe a considerable fraction ($\sim 60\%$) of the total number of supra-thermal stars even when the binary is very hard ($a \leq 4$ AU).

For completeness, we also considered a third timescale: the gravitational wave timescale, t_{gw} , i.e. the characteristic time for a binary IMBH to coalesce due to gravitational wave emission. When this timescale, defined as (Peters 1964; Quinlan 1996)

$$t_{gw} = \frac{5}{256} \frac{c^5 a^4 (1 - e^2)^{7/2}}{G^3 M_1 M_2 (M_1 + M_2)}, \quad (7)$$

becomes shorter than t_{hard} , the binary would shrink, due to gravitational wave emission, at a rate shorter than what we expected from t_{hard} . Figure 6 shows the timescale t_{gw} computed for a constant eccentricity $e = 0.7$ (the initial eccentricity we chose for our runs) and for the range of masses considered in this paper. We expect that the assumption of constant eccentricity is correct for star-binary IMBH interactions, since, when $M_1 + M_2 \gg m$, the binary eccentricity suffers very small changes. We also checked whether this assumption is correct on the basis of our simulations. We found that the mean eccentricity e of the binary IMBH after a 3-body encounter is always 0.70, with a very narrow spread (the standard deviation σ being always $1 - 5 \times 10^{-2}$), and the maximum post-encounter eccentricity is always $\lesssim 0.8$, in agreement with our statement.

From Figure 6 we note that t_{gw} is longer than t_{hard} , for $a \gtrsim 0.5 - 0.3$ AU. This implies that the lifetime of a binary IMBH is controlled by 3-body scattering on the hardening time t_{hard} , as long as the binary separation $a \sim 0.1$ AU. Therefore, we can neglect the effect of gravitational wave emission, since we consider binaries wider than 0.1 AU.

The second condition concerns the number of supra-thermal stars: their total should be large enough in order to observe a sizable fraction of them in the cluster halo. The total number N of stars interacting with a binary is given by (cfr. CMP):

$$N = \frac{(M_1 + M_2)}{m \xi_E} \ln \left(\frac{a_0}{a_{st}} \right) \quad (8)$$

where a_0 is the initial semi-major axis of the binary and a_{st} is the minimum semi-major axis for the encounter to give a supra-thermal star. A fraction f of the number N gives the number of supra-thermal stars. Reaching distances from the GC core greater than those of all the other stars that suffered an interaction, they can be easily detectable: in fact, at the periphery of the cluster where the relaxation time is longer, the supra-thermal stars need more time than the average to return back to the core and in addition are surrounded by stars with considerable lower systemic velocities. We derive N from equation (8), where we impose $a_0 = 2000$ AU, corresponding to the orbital separation below which the binary becomes reasonably hard to generate supra-thermal

Table 6. Statistics for initially counterrotating bound stars^a.

	Corot _{fin} (%) ^b	Counterrot _{fin} (%) ^c	More aligned stars (%) ^d	$J_*^{fin} > J_*^{in}$ (%) ^e
CASE A1	7	93	54	60
CASE A2	43	57	75	69
CASE A3	57	43	81	85
CASE A4	21	79	58	57
CASE B1	3	97	49	57
CASE B2	57	43	79	60
CASE B3	56	44	77	82
CASE B4	55	45	79	55
CASE C1	34	66	52	57
CASE C2	23	76	68	57
CASE C3	39	61	79	84
CASE C4	17	83	57	58
CASE D1	6	94	52	61
CASE D2	54	46	78	76
CASE D3	67	33	84	97
CASE D4	62	38	83	71
CASE E1	5	95	52	59
CASE E2	15	85	69	59
CASE E3	13	87	85	90
CASE E4	15	85	65	57

^a In this Table we consider only the stars which before the interaction were counterrotating.

^b Percentage (respect to the total of initially counterrotating bound stars) of stars which, after the interaction, become corotating with the binary.

^c Percentage (respect to the total of initially counterrotating bound stars) of stars which, after the interaction, remain counterrotating respect to the binary.

^d Percentage (respect to the total of initially counterrotating bound stars) of stars which, after the encounter, reduce the angle between their angular momentum and that of the binary.

^e Percentage of bound stars (respect to the total of initially counterrotating bound stars) which, after the encounter, increase the absolute value of their angular momentum.

stars, and $a_{st} = 0.1$ AU, the orbital separation below which the cross section for 3-body encounters becomes negligible. We then calculate the number of stars that remain bound to the cluster and the number of supra-thermal stars using the statistics derived in our simulations (see the percentages given in Table 3, respectively in first column -for the bound stars- and in fourth column -for the supra-thermal). The results are shown in Table 7. The total number of bound stars is always greater than 400 and the number of stars stirred up to supra-thermal velocities is always greater than 100, even for the lightest system ($M_1 = 50 M_\odot$, $M_2 = 10 M_\odot$).

Supra-thermal stars should be observable from their proper motion and/or Doppler line shift. To quantify the fraction of supra-thermal stars which can be detected, we have to take into account projection effects. Estimating these projection effects from the outputs of our simulations, we find that in all cases near 80% of supra-thermal stars should really be detectable as stars with projected velocity higher than $20/f_{pr}$ km s⁻¹ (where f_{pr} , the projection factor, is $\sqrt{3}$ for Doppler measurements and $\sqrt{3/2}$ for proper motions). Assuming this percentage (we will discuss later its validity limits), we find that the number of observable supra-thermal stars over the entire cluster is $\gtrsim 100$ for a "light" binary IMBH ($M_1 = 50 M_\odot$, $M_2 = 10 M_\odot$) and $\gtrsim 200$ for a "moderately massive" binary IMBH ($M_1 = 100 M_\odot$, $M_2 = 50 M_\odot$).

And what about the detection of the angular momentum alignment effect? Column 2 of Table 4 tells us that in the most favorite case about 70% of the stars which remain bound are corotating with the binary IMBH, whereas 30% are counterrotating. We also noticed that these percentages are nearly the same if we consider not all the bound stars, but only the supra-thermal stars. This means that, if there is a binary IMBH of $M_1 = 100 M_\odot$ and $M_2 = 50 M_\odot$, we should have about 180 corotating and only 80 counterrotating supra-thermal stars. To calculate how many of these corotating and counterrotating stars are observable as supra-thermal stars, we have to take into account the projection effects. As said, about 80% of supra-thermal stars are in average detectable as such. Unfortunately this estimate is an upper limit. In the runs where supra-thermal stars gain angular momentum from the binary IMBH, so that there is also significant alignment (case A3, C3, D3 and D4), the fraction of observable supra-thermal stars is 80-85% only when the line-of sight happens to be nearly parallel to the orbital angular momentum of the binary IMBH \mathbf{J}_{BH} , if we are measuring proper motions (or when the line-of-sight is nearly perpendicular to \mathbf{J}_{BH} , if we are measuring Doppler-shifts). If, on the contrary, we are in the most unlucky cases (that is when the line of sight happens to be nearly perpendicular to the orbital angular momentum of the binary IMBH \mathbf{J}_{BH} and we are measuring supra-thermal velocity

Table 7. Number of supra-thermal stars^a

M_1^b	M_2^b	Interacting stars ^c	Bound stars ^d	Supra-thermal stars	Supra-thermal stars (last 2 Gyrs) ^e
50	10	728	467	128	86
50	50	1651	1009	219	146
100	10	2060	1567	238	157
100	50	1722	727	262	158
200	10	1945	1057	306	176

^a These numbers are calculated for binaries having $a_0 = 2000$ AU and $a_{st} = 0.1$ AU

^b In units of solar masses. M_1 and M_2 represent respectively the mass of the more and of the less massive black hole in the binary IMBH.

^c Total number of stars which have an interaction with the binary IMBH.

^d Number of stars which after the interaction remain bound to the cluster.

^e Supra-thermal stars formed in the last 2 Gyrs.

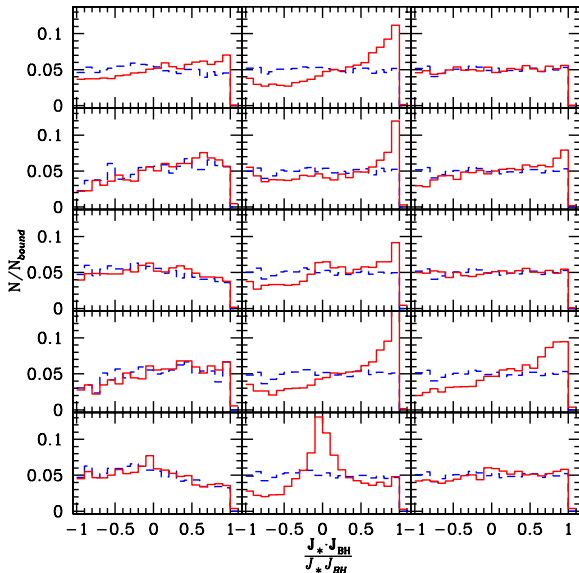


Figure 5. The histograms show the distribution of $\frac{\mathbf{J}_* \cdot \mathbf{J}_{BH}}{J_* \cdot J_{BH}}$ for all the considered cases. *Solid line* indicates the distribution after the encounter; *dashed line* indicates the distribution before the encounter. From the up left panel, going toward right: case A2, A3, A4, B2, B3, B4, C2, C3, C4, D2, D3, D4, E2, E3, E4. We do not plot cases A1, B1, C1, D1 and E1 because they are similar to cases A2, B2, C2, D2 and E2. On the y-axis the number of cases for each bin is normalized to the total number of bound stars (N_{bound}).

from proper motions, or when the line of sight is parallel to \mathbf{J}_{BH} and we are measuring Doppler shifts), the fraction of detectable supra-thermal stars reduces respectively to 55% and 40%. Taking into account these extreme cases, in presence of a binary IMBH of $M_1 = 100 M_\odot$ and $M_2 = 50 M_\odot$ we should detect about 70-100 corotating and 30-40 counterrotating stars. In summary, taking into accounts projection effects and instrumental characteristics, we expect to observe, for a binary IMBH of $(100M_\odot, 50M_\odot)$, from 100 to 220 supra-thermal stars.

To derive the effective number of detectable supra-thermal stars, we have to take into account other factors.

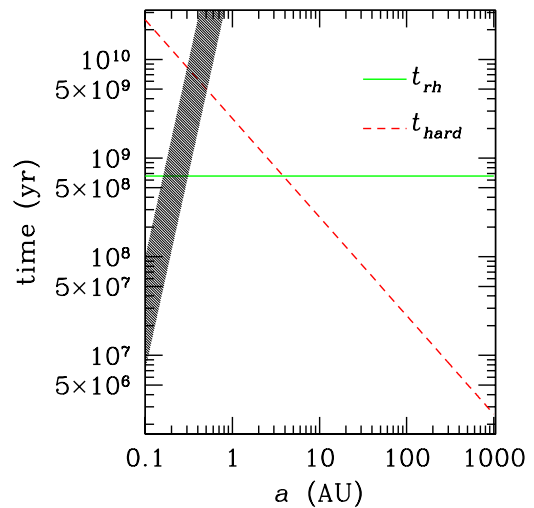


Figure 6. Half mass relaxation time, t_{rh} , and hardening time, t_{hard} , as a function of the initial orbital separation a (in AU) of the binary IMBH, for $n = 10^5 \text{ pc}^{-3}$, $\xi_E = 1$, and $\sigma = 8.5 \text{ km s}^{-1}$. The shaded area indicates the gravitational wave timescale t_{gw} for binary IMBHs in the considered range of masses (from 60 to 210 M_\odot) and with eccentricity $e = 0.7$.

First of all, this estimate refers to all stars, considering also compact remnants (neutron stars, white dwarfs) and stellar types which are not easily observable, being too faint. Red giants, which are the most easily detectable stars in GCs tracing the light, are only 10% of the total population of stars and remnants, even if this percentage increases in the core, because of mass segregation. We are also able to detect horizontal branch (HB) stars and main sequence (MS) stars of sufficiently high mass ($m \gtrsim 0.6 M_\odot$). Using the numerical code which will be described in the next Section, we find that the stars with mass from 0.6 to 0.9 M_\odot (a mass range which includes red giant, HB and detectable MS stars) rep-

resent about the 45% of the stars enclosed within¹ $0.1 r_c$ of a GC like NGC 6752. This means that, in the case of a binary of $(100M_\odot, 50M_\odot)$, we are able to detect only 50-100 supra-thermal stars.

There is an additional problem concerning the detection of supra-thermal stars. Nearly all the proposed mechanisms of formation of binary IMBHs in GCs (Miller & Hamilton 2002; Sigurdsson & Hernquist 1993) predict that such binaries are born within the first Gyr since the formation of the GC itself. If this is true, considering the hardening time t_{hard} plotted in Figure 6, the binary IMBHs which still survive today must have orbital separation $\lesssim 1$ AU (for a cluster with $n = 10^5 \text{ pc}^{-3}$). This means that all the supra-thermal stars produced when the binary had orbital separation $a \gtrsim 3$ AU have already been thermalized, because a time much longer than t_{rh} has elapsed (Fig. 6). Then, we can observe only the supra-thermal stars produced in the last ~ 2 Gyr (about $3 t_{rh}$, because a supra-thermal star can have apo-center distance larger than the half mass radius and, therefore, relaxation time longer than t_{rh}). Luckily, the orbital separation of a IMBH binary remains in the range 0.1-3 AU for a long time, because the hardening rate is lower for such a hard binary, and a large fraction of supra-thermal stars ($\sim 60\%$) is produced in this stage. The number of these "surviving" supra-thermal stars is reported in Table 7, 6th column. Let us consider again the IMBH binary of $(100,50) M_\odot$. The total number of supra-thermal stars produced by this binary in the last 2 Gyrs is ~ 160 . This means that, taking into account projection effects and considering that we can observe only stars in the mass range $0.6-0.9 M_\odot$, we can detect only 30-60 supra-thermal stars.

On the other hand, angular momentum alignment effects are visible only for sufficiently wide binaries ($a > 10$ AU). Thus, unless a binary IMBH is formed recently in a cluster, the alignment effect today is completely washed out by dynamical friction.

For completeness, we notice that a very low probability mechanism of binary IMBH formation in GCs in recent epochs exists. In fact, there is some possibility that a "last single BH" (Sigurdsson & Hernquist 1993), ejected from the core in the early stages of the GC life, remains in the halo for several Gyrs. The relaxation timescale out in the halo is long, and if the orbits can circularize there (maybe due to time varying galactic tidal field), then the return time to the core is long. When this BH comes back to the core, there is a high probability that it forms a binary with the central IMBH. Such a binary IMBH would be originate in late epochs. However, the probability for this process to occur is low, because it requires the BH to receive just the fine-tuned post-encounter velocity needed to remain in the outer halo: if the velocity is slightly too high, the BH will be ejected from the entire cluster; whereas, if the velocity is low, the return time to the core will be too short.

Therefore, if we exclude the remote possibility that the binary IMBH is formed in the last few Gyrs, we have to conclude that the angular momentum alignment by a hypo-

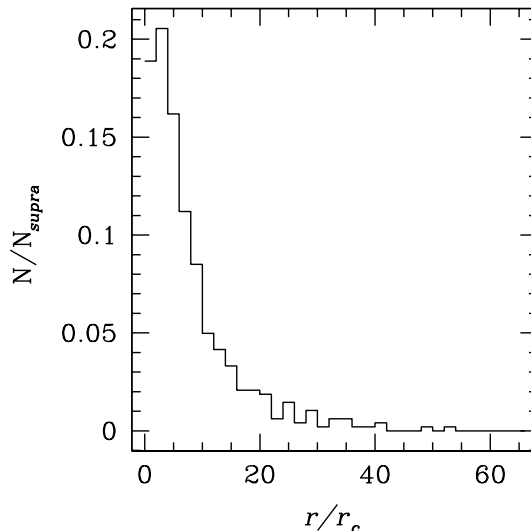


Figure 7. Final projected distribution of the high velocity supra-thermal stars in the case D3. The peak is at $3 r_c$. On the y-axis the number of cases for each bin is normalized to the total number of supra-thermal stars (N_{supra}).

thetical IMBH does not persist in GCs today and that even the detection of supra-thermal stars is very difficult.

4.2 Spatial distribution of the supra-thermal stars

As shown in the previous Sections, a binary IMBH, during its hardening, produces a certain number of supra-thermal stars, which, once detected, could indirectly reveal its presence. These supra-thermal stars are only few tens; but their detection remains still possible, if their radial distribution shows some characteristic feature. Thus, it is of interest to study how supra-thermal stars evolve in the cluster and what is their radial distribution.

To this purpose we have explored the dynamics of supra-thermal stars in a cluster under the action of dynamical friction and the influence of two-body relaxation effects using an updated version of the code described in Sigurdsson & Phinney 1995. The code first generates a cluster background model, i.e. a multi-mass King density profile which in our case reproduces that of NGC 6752, and we inject in this background supra-thermal stars whose initial velocities are those obtained by our 3-body simulations. We followed the dynamical evolution of these stars for a random time t uniformly distributed in the range $0 < t \leq 3 t_{rh}$. In this way we can see how supra-thermal stars distribute in the cluster before thermalization. After evolution for a time $t \lesssim 3 t_{rh}$ we select the stars that still are supra-thermal. We applied this procedure to the cases D1, D2, D3 and D4.

The stars which were still supra-thermal when the simulation stopped and that can be observed as supra-thermal, taking into account two-dimensional (one-dimensional) projection effects and ejections, are about 70% (60%) of the initial sample. These stars present a radial distribution like that shown in Figure 7 (for the case D1). This distribution is

¹ We consider the region within $0.1 r_c$, because we are interested in those stars which have the highest probability of interacting with the central binary IMBH.

strongly peaked around a radius r_{peak} which is of the order of few core radii for all the considered systems.

The key question is whether this peak can be detected by current generation of instruments. Let consider the binary with $M_1 = 100 M_\odot$, $M_2 = 50 M_\odot$ and $a = 1$ AU (D1). In this case $r_{peak} = 3 r_c$ for NGC 6752. To establish if this peak is significant we used a Poissonian estimate, that is we checked if

$$N_{peak} - \sqrt{N_{peak}} > \langle N \rangle + \sqrt{\langle N \rangle} \quad (9)$$

where N_{peak} is the number of high velocity supra-thermal stars in the bin centered at $r_{peak} = 3 r_c$ and $\langle N \rangle$ is the average number of high velocity supra-thermal stars in the other bins².

We found that, taking into account both projection effects and the fact that only stars with masses from ~ 0.6 to $\sim 0.9 M_\odot$ are observable, $N_{peak} \sim 10$ and $\langle N \rangle \sim 1$. Thus, the effect is significant. But this consideration would be valid only if we were able to map all the GC surface ranging from 0 to $80 r_c$. Because this seems unlikely, we calculated what is the minimum area which has to be observed to make significant the relation (9). We found that, to have statistical evidence of the peak of supra-thermal stars, it is sufficient to measure radial velocities within a distance of $6 r_c$ from the cluster center, an observational issue which seems possible for clusters like NGC 6752.

On the other hand, taking again into account both projection effects and the fact that only stars with masses from ~ 0.6 to $\sim 0.9 M_\odot$ are observable, we expect to detect ~ 50 supra-thermal stars in the entire cluster (see Section 4.1), ~ 27 of which are located within $6 r_c$. This number is so small that we also checked whether it is comparable with the number of high velocity stars predicted by the equilibrium (e.g. Maxwellian) velocity distribution. In particular, we derived the number of stars with mass from 0.6 to $0.9 M_\odot$ and with velocity in the supra-thermal range (between 20 and 40 km s⁻¹) which are expected to be within $6 r_c$ of NGC 6752 (core density $n \sim 2 \times 10^5$ stars pc⁻³, central projected velocity dispersion $\sigma_{1D} = 4.9$ km s⁻¹) assuming a Maxwellian velocity distribution. We found that, if the velocity distribution is Maxwellian, ~ 10 stars with velocity in the supra-thermal range are predicted to inhabit within a distance of $6 r_c$ from the center of NGC 6752. Then, the number of supra-thermal stars produced by interactions with a binary IMBH should be dominant with respect to the high velocity tail of the Maxwellian distribution; the presence of this tail further dilutes the signature of supra-thermal stars.

4.3 What about binary SMBHs?

In this paper we focused on binary IMBHs. Nonetheless, it would be of interest to ask whether supra-thermal stars and angular momentum alignment are effects visible in galactic nuclei, around binary supermassive black holes (SMBHs). In fact, in contrast to the case of IMBHs, there is clear evidence of the existence of double active nuclei, i.e., accreting SMBH pairs in merging galaxies (Komossa et al. 2003) that may end their dynamical evolution in the form of a close Keplerian binary (Kazantzidis et al. 2005). In principle, there

is nothing which forbids us to extend our findings to 3-body encounters of stars with with binary SMBHs. In practice, we would need specific simulations to verify if our assumptions are correct also for binary SMBHs in galactic bulges. However, we can roughly extrapolate our results to the case of SMBHs.

Applying equation 8 to the case of a binary SMBHs with $(M_1 + M_2) = 10^7 M_\odot$, $a_0 = 2$ pc, $a_{st} = 0.1$ pc and $m = M_\odot$, we obtain that such binary experiments about 7.7×10^6 stellar encounters. Assuming that the fraction of stars which, after the encounter, are supra-thermal and remain bound to the bulge is at least 40% (because the escape velocity from the bulge is much higher than in GCs), we should observe more than 3×10^6 supra-thermal stars in the neighborhoods of the galaxy center. If the two SMBHs have similar masses (which seems to be the case of NGC 6240, Komossa et al. 2003), the fraction of supra-thermal stars which should be corotating with the orbital plane of the two SMBHs can be about 60-70%. Then we should have about 2×10^6 corotating stars and about 1×10^6 counterrotating stars. Obviously this result suffers of dramatic simplifications and one must be careful in considering it. With this very rough calculation we wanted only to suggest that dedicated works should be carried on, exploring the velocity and angular momentum distribution of stars involved in 3-body encounters with binary SMBHs.

5 SUMMARY

In our work we explored the effects that the presence of a binary IMBH imprints on the velocity and angular momentum of cluster stars, due to 3-body encounters with it. The main results of our analysis can be summarized as follows.

- (i) A binary IMBH generates a family of supra-thermal stars, i.e. of stars which remain bound to the cluster, but have a velocity higher than the dispersion velocity. (§ 3.1).
- (ii) A fraction of stars tend to align their angular momentum, \mathbf{J}_* , with that of the binary IMBH, \mathbf{J}_{BH} . This fraction depends on the reduced mass μ and on the semi-major axis a of the binary IMBH, but it is always of the order of 55-70%. This means that the angular momentum distribution of stars that have suffered 3-body interaction with a binary IMBH presents a slight anisotropy (§ 3.2).

(iii) But are these supra-thermal stars really detectable? In a GC hosting a binary IMBH we expect few hundreds of supra-thermal stars. Only $\sim 45\%$ of them are detectable, once subtracted the fraction of compact remnants and faint stars. Further, we have to take into account projection effects. The result is that we expect to observe, in the best cases, about one hundred of supra-thermal stars (§ 4.1). It can be interesting to notice that there is already a claim for the detection of high velocity stars in 47 Tuc (Meylan, Dubath & Mayor 1991).

(iv) The present theoretical models of binary IMBH formation indicate that these systems are produced in the first Gyr of the GC life. This means that today, in dense clusters like NGC 6752, binary IMBHs have, due to hardening, orbital separation $a \lesssim 1$ AU. As a consequence, supra-thermal stars produced when the binary was wider have already thermalized. Then, we can only observe supra-thermal stars formed in the last 2 Gyrs, which are about the 60% of

² The bins are the same shown in Fig. 7. Each bin is wide $2 r_c$.

the total (§ 4.1). These "surviving" supra-thermal stars do not show any signature of angular momentum alignment, because this effect is evident only when the stars interact with a relatively wide binary ($a > 10$ AU).

(v) Detectable supra-thermal stars seem to be a very small number ($\lesssim 100$ in the entire cluster), unless binary IMBHs also form in the last Gyrs. Therefore, it is particularly important to study the expected radial distribution of supra-thermal stars, searching for characteristic features which can make easier their detection. To this purpose, we followed the dynamical evolution of supra-thermal stars in the cluster potential (assuming a cluster model which reproduces the observational characteristics of NGC 6752), taking into account dynamical friction and two body relaxation. We found that, before thermalization, supra-thermal stars tend to cluster within $4 r_c$. We showed that it is sufficient to measure radial velocities within $6 r_c$, in order to have statistical evidence of the presence of supra-thermal stars (§ 4.2).

In the light of these findings, the search of supra-thermal stars and of anisotropies in their angular momentum distribution can provide, in principle, useful indications on the existence of binary IMBHs in GCs. However, the detection of the signature left by a binary IMBH on the velocity field of stars in a cluster may be a challenge for present instrumentation, but it may become a relatively trivial task for future telescopes having much bigger collecting area, like (Gilmozzi 2004) the Thirty Meter Telescope (TMT) or the Overwhelmingly Large Telescope (OWL).

6 ACKNOWLEDGMENTS

We thank Francesco Ferraro for useful discussions on the issue of supra-thermal star detection, and Cole Miller for a critical reading of the manuscript. This work found first light during the workshop "Making Waves with Intermediate-Mass Black Holes" (20-22 May 2004, Penn State University). M. C. and M. M. acknowledge the Center for Gravitational Wave Physics for kind hospitality. S. S. acknowledges support by the Center for Gravitational Wave Physics funded by the NSF under cooperative agreement PHY 01-14375 and NSF grant PHY 02-03046. M. C. and A. P. acknowledge financial support from the MURST, under PRIN03.

REFERENCES

Abel T., Bryan G. L., Norman M. L., 2002, *Sci*, 295, 93
 Belczynski K., Bulik T., Rudak B., 2004, *ApJL*, 608, 45
 Camilo F., Rasio F. A., 2005, *ASP Conf. Ser. Vol. 328*, 2005: Binary Radio Pulsars, eds. F. A. Rasio, I. H. Stairs, *astro-ph/0501226*
 Colpi M., Devecchi B., Mapelli M., Patruno A., Possenti A., 2005, *astro-ph/0504198*, Invited review in: "Interacting binaries", July 4-10 Cefalu, eds. Antonelli et al., to be published with AIP
 Colpi M., Mapelli M., Possenti A., 2004, *Coevolution of Black Holes and Galaxies*, from the Carnegie Observatories Centennial Symposia. Carnegie Observatories Astrophysics Series. Edited by L. C. Ho, 2004.
<http://www.ociw.edu/ociw/symposia/series/symposium1/proceedings.html>
 Colpi M., Mapelli M., Possenti A., 2003, *ApJ*, 599, 1260

Colpi M., Possenti A., Gualandris A., 2002, *ApJL*, 570, 85
 D'Amico N., Possenti A., Fici L., Manchester R. N., Lyne A. G., Camilo F., Sarkissian J., 2002, *ApJL*, 570, 89
 Dubath P., Meylan G., Mayor M., 1997, *A&A*, 324, 505
 Fabbiano G., 2004, *Compact Binaries in the Galaxy and Beyond*, Proceedings of the conference held 17-22 November, 2003 in La Paz, Baja California Sur. Edited by G. Tovmassian and E. Sion. *Revista Mexicana de Astronomia y Astrofisica (Serie de Conferencias)* Vol. 20. IAU Colloquium 194, pp. 46-49
 Ferraro F. R., Possenti A., Sabbi E., D'Amico N., 2003, *ApJL*, 596, 211
 Ferraro F. R., Possenti A., Sabbi E., Lagani P., Rood R. T., D'Amico N., Origlia L., 2003, *ApJ*, 595, 179
 Fregeau J. M., Cheung P., Portegies Zwart S. F., Rasio F. A., 2004, *MNRAS*, 352, 1
 Freitag M., Rasio F. A., Baumgardt H., 2005a, *astro-ph/0503129*
 Freitag M., Gürkan M. A., Rasio F. A., 2005b, *astro-ph/0503130*
 Gebhardt K., Pryor C., Williams T. B., Hesser J. E., 1995, *AJ*, 110, 1699
 Gebhardt K., Pryor C., Williams T. B., Hesser J. E., Stetson P. B., 1997, *AJ*, 113, 1026
 Gebhardt K., Pryor C., O'Connell R. D., Williams T. B., Hesser J. E., 2000, *AJ*, 119, 1268
 Gebhardt K., Rich R. M., Ho L. C., 2002, *ApJL*, 578, 41
 Gerssen J., van der Marel R. P., Gebhardt K., Guhathakurta P., Peterson R. C., Pryor C., 2003, *AJ*, 125, 376
 Gerssen J., van der Marel R. P., Gebhardt K., Guhathakurta P., Peterson R. C., Pryor C., 2002, *AJ*, 124, 3270
 Gilmozzi R., 2004, *SPIE*, 5489, in press
 Gultekin K., Miller M. C., Hamilton D. P., 2004, *astro-ph/0402532*, submitted to *ApJ*
 Gürkan M. A., Freitag M., Rasio F. A., 2004, *ApJ*, 604, 632
 Heger A., Fryer C. L., Woosley S. E., Langer N., Hartmann D. H., 2003, *ApJ* 591, 288
 Hut P., Bahcall J. N., 1983, *ApJ*, 268, 319
 Kazantzidis S., et al., 2005, *ApJL*, 623, 67
 Komossa S., Burwitz V., Hasinger G., Predehl P., Kaastra J. S., Ikebe Y., 2003, *ApJL* 582, 15
 Kulkarni S. R., Hut P., McMillan S., 1993, *Natur*, 364, 421
 Madau P., Rees M. J., 2001, *ApJL*, 551, 27
 Meylan G., Dubath P., Mayor M., 1991, *ApJ*, 383, 586
 Miller M. C., 2002, *ApJ*, 581, 438
 Miller M. C., Hamilton D. P., 2002, *MNRAS*, 330, 232
 Mushotzky R., 2004, *Progress of Theoretical Physics Supplement*, 155, 27
 Orosz J. A., 2003, *astro-ph/0209041*, invited talk at IAU Symp. 212, "A Massive Star Odyssey, from Main Sequence to Supernova", to appear in the proceedings (K. A. van der Hucht, A. Herrero, & C. Esteban eds., San Francisco: ASP)
 Peters P. C., 1964, *Phys. Rev.* B136, 1224
 Phinney E. S., 1993, *Structure and Dynamics of Globular Clusters*. Proceedings of a Workshop held in Berkeley, California, July 15-17, 1992, to Honor the 65th Birthday of Ivan King. Editors, S.G. Djorgovski and G. Meylan; Publisher, Astronomical Society of the Pacific, Vol. 50, San Francisco, California
 Portegies Zwart S. F., 2004, *astro-ph/0406550*, Lecture note to appear in "Joint Evolution of Black Holes and Galaxies" of the Series in High Energy Physics, Cosmology and Gravitation. IOP Publishing, Bristol and Philadelphia, 2005, eds M. Colpi, V. Gorini, F. Haardt and U. Moschella ...
 Portegies Zwart S. F., Baumgardt H., Hut P., Makino J., McMillan S. L. W., 2004, *Natur*, 428, 724
 Portegies Zwart S. F., McMillan S. L. W., 2002, *ApJ*, 576, 899
 Portegies Zwart S. F., McMillan S. L. W., 2000, *ApJL*, 528, 17
 Possenti A., 2003, *Radio Pulsars*, ASP Conference Proceedings, Vol. 302. Held 26-29 August 2002 at Mediterranean Agronomic Institute of Chania, Crete, Greece. Edited by Matthew

- Bailes, David J. Nice and Stephen E. Thorsett. San Francisco:
Astronomical Society of the Pacific
- Quinlan G. D., 1996, *NewA*, 1, 35
- Ransom S. M., Hessels J. W. T., Stairs I. H., Freire P. C. C.,
Camilo F., Kaspi V. M., Kaplan D. L., 2005, *Sci*, 307, 892
- Schneider R., Ferrara A., Natarajan P., Omukai K., 2002, *ApJ*,
571, 30
- Sigurdsson S., Hernquist L., 1993, *Natur*, 364, 423
- Sigurdsson S., Phinney E. S., 1995, *ApJS*, 99, 609
- Sigurdsson S., Phinney E. S., 1993, *ApJ*, 415, 631
- van der Marel R. P., 2004, *Coevolution of Black Holes and
Galaxies, from the Carnegie Observatories Centennial Sym-
posia*. Published by Cambridge University Press, as part of
the Carnegie Observatories Astrophysics Series. Edited by
L. C. Ho
- Volonteri M., Haardt F., Madau P., 2003, *ApJ*, 582, 559